Astron. Astrophys. 321, 811–821 (1997)

ASTRONOMY AND ASTROPHYSICS

Time-series photometric spot modeling

III. Thirty years in the life of HK Lacertae

K. Oláh[1], **Zs. Kővári**[1], **J. Bartus**[1,2], **K.G. Strassmeier**[2], **D.S. Hall**[3], **and G.W. Henry**[4]

[1] Konkoly Observatory of the Hungarian Academy of Sciences, H-1525 Budapest, Hungary
(olah@ogyalla.konkoly.hu, kovari@buda.konkoly.hu, bartus@buda.konkoly.hu)
[2] Institut für Astronomie, Universität Wien, Türkenschanzstraße 17, A-1180 Wien, Austria (strassmeier@astro.ast.univie.ac.at)
[3] Dyer Observatory, Vanderbilt University, Nashville, TN 37235, USA (hallxxds@ctrvax.vanderbilt.edu)
[4] Center for Automated Space Science and Center of Excellence in Information Systems, Tennessee State University, Nashville, TN 37203-3401, USA (henry@coe.tnstate.edu)

Received 2 September 1996 / Accepted 5 November 1996

Abstract. We present a spot modeling analysis of the active late-type giant HK Lac using 30 years of photometry, including 600 new data points from the last six years. We have analyzed folded light curves and, when we had long continuous data sets, applied a new computer code for time-series modeling. The validity of the modeling results was tested as a function of the photometric noise. We have determined the unspotted brightness of HK Lac in the $BV(RI)_C$ bandpasses and obtained a spot temperature of ΔT = 1200 $\pm$ 100 K. Polar active regions were recovered throughout the modeling because no other scenario was able to describe both the mean light variability of over $0\overset{\mathrm{m}}{.}25$ accompanied by rotational modulation of similar amplitude. This result has gotten strong theoretical support recently (see Schüssler 1996). The active regions preferably cluster around two orbital phases separated by $\approx 110°$. New spot appearences within active regions and, possibly, their interactions with the old ones could be the cause of rapid changes in the light curves.

Key words: stars: activity – stars: late-type – stars: individual: HK Lac – stars: spots

1. Introduction

The active, long-period binary system HK Lacertae (HD 209813, $P_{\rm orb}$ = 24 days, K0III) is one of the most well-observed long-period RS CVn stars and nearly continuous photometry exists since the discovery of its light variability in 1967 (Blanco & Catalano 1970). Basic stellar and orbital parameters of HK Lacertae are given in the second edition of the "Catalog of Chromospherically Active Binary Stars" (CABS, Strassmeier et al. 1993). The photometric history up to 1985 has been summarized by Oláh et al. (1985).

More recently, Mitrou et al. (1995) reported colour-corrected IRAS magnitudes of HK Lac of $m_{12\mu} = 4\overset{\mathrm{m}}{.}07$ and $m_{25\mu} = 4\overset{\mathrm{m}}{.}04$ and assumed $V_{\rm max} = 6\overset{\mathrm{m}}{.}52$. Estalella et al. (1993) observed the star at 3.6 cm radio wavelength that resulted in four non-detections and one detection with 12±6 mJy. At 6 cm Drake et al. (1992) measured a flux density of 4.57±0.07 mJy and a circular polarization of –6.2%. Dempsey et al. (1993a,1993b) found an X-ray luminosity of $L_{\rm x}$ = 31.23 erg s^{-1} from the ROSAT all-sky survey and obtained a two-temperature spectral fit with $T_{\rm high}$=2.02×10^7 K and $T_{\rm low}$=1.85×10^6 K. Ca II H&K emission-line fluxes were measured by Fernández-Figueroa et al. (1994) and were converted to flux at the Earth of $F_{\rm obs}$(K)=3.18×10^{-12} erg cm^{-2}s^{-1} and $F_{\rm obs}$(H)=2.81×10^{-12} erg cm^{-2}s^{-1}. In the ultraviolet, Mg II h&k emission-line variability was detected and seen in anticorrelation with the V-band light curve (Oláh et al. 1992) with an average net flux at the Earth of about 12×10^{-12} erg cm^{-2}s^{-1}.

A six days long flare event in Hα was observed on HK Lac in 1989 (Catalano & Frasca, 1994), possibly connected with the emergence of a new spot (Oláh et al. 1991). Another Hα flare-like event was observed in 1994 (Catalano et al. 1996).

It will be seen that the spot modeling analysis we use here rests heavily upon two assumptions which end up being critically responsible for several major features of the resulting starspot maps. One assumption is that there are only two spots; the other is that we can correctly identify the brightness of an unspotted hemisphere. If either of these assumptions were to be relaxed, the case for the two very large, virtually permanent, oppositely situated, high-latitude (polar) spots would be much less compelling. For recent discussion of light curve modeling with more than two spots and the question of the unspotted hemisphere, see Eaton et al. (1996).

Send offprint requests to: K. Oláh

In this investigation we present a self-consistent spot modeling analysis of broad-band, multi-color photometry using all existing photometric data up to 1996 including the original data from the discovery of the light variability of HK Lac by Blanco & Catalano (1970) as well as subsequent photometry by Herbst (1973), Vogt (1981), Percy & Welch (1982), Poe & Eaton (1985), Oláh & Hall (1988) and Derman et al. (1990). The technique of time-series spot modeling has been described in the first paper in this series where we also applied it to VY Arietis = HD 17433 (Strassmeier & Bopp 1992), hereafter paper I, and to V1762 Cyg = HR 7275 (Strassmeier et al. 1994, paper II).

2. Observations

The new observations in this paper were obtained mostly with the Vanderbilt-Tennessee State APT (automatic photoelectric telescope) on Mount Hopkins, Arizona (Henry 1995a, 1995b) in the years 1986 and 1996. Part of the data from 1986–89 have already been analysed in a previous paper (Oláh et al. 1992), but we have nearly 600 new data points observed mostly in Johnson B and V. Additionally, 86 $UBV(RI)_C$ data points were obtained at Piszkéstető (mountain station of Konkoly Observatory) between 1988–1992 with the 1 m telescope equipped with a thermoelectrically cooled photon-counting photometer.

All light curves in this paper were phased with the orbital ephemeris of Gorza & Heard (1971):

$$2,440,017.170 \pm 0.054 + 24.4284 \pm 0.0005 \times E. \quad (1)$$

All published photometry of HK Lac used either HD 208728 or HD 210731 as the comparison star, and different observers generally gave their data with respect to the one or the other. We arranged all data so that the magnitude differences are always with respect to HD 210731. For this purpose we applied the average of 67 differential measurements of the two comparison stars as observed in $UBV(RI)_C$ at Konkoly Observatory. These averages are in the sense of HD208728 minus HD210731 and are as follows: $\Delta U = 0\overset{\mathrm{m}}{.}7265 \pm 0\overset{\mathrm{m}}{.}0025$; $\Delta B = -0\overset{\mathrm{m}}{.}0005 \pm 0\overset{\mathrm{m}}{.}0025$; $\Delta V = -0\overset{\mathrm{m}}{.}6011 \pm 0\overset{\mathrm{m}}{.}0001$; $\Delta R_C = -0\overset{\mathrm{m}}{.}9271 \pm 0\overset{\mathrm{m}}{.}0005$; $\Delta I_C = -1\overset{\mathrm{m}}{.}2017 \pm 0\overset{\mathrm{m}}{.}0012$.

3. The applied spot modeling technique

3.1. Adopted parameters and assumptions

The moderate space motion of HK Lac, U= -47.5 km/s, V= -29.6 km/s, W= -3.9 km/s, (CABS, Strassmeier et al. 1993) suggests that it is an intermediate-age disk-population system (not pop I), thus the mass of the K0III star should be less than 1.5 $M_\odot$. We adopt $i = 68°$ for the inclination of the rotational axis as recently determined by Stawikowski & Glebocki (1994) from $P_{\rm rot}$ and $V_{\rm rot} \sin i$ assuming $R_1 = 12$ $R_\odot$. Thus, the mass function of $f(m) = 0.105$ (Gorza & Heard 1971) leads to a G5V secondary with $M_V \approx 5.1$, $M_2 \approx 0.92 M_\odot$, $T_{\rm eff} \approx 5770$ K and $R_2 \approx 0.92$ $R_\odot$ (Schmidt-Kaler 1982). From an upper estimation of the primary radius of 16 $R_\odot$ (while the system is still noneclipsing) the light curve should show a double sine variability with $\approx 0\overset{\mathrm{m}}{.}06$ amplitude due to the expected tidal distortion of the giant star (i.e. ellipticity effect). However, this effect is not seen when examining the light curves at high system brightness/low spottedness. We thus assume the radius of the giant component to be $R_1 \leqq 12$ $R_\odot$ (in agreement with an observed line broadening of $V \sin i = 23$ km/s, see Randich et al. 1994) and a neglectable ellipticity effect.

Table 1. Fixed light curve parameters

Bandpass	flux ratio spot/phot*	limb darkening	unspotted light (Δmag)
B	0.105	0.899	-0.300
V	0.165	0.743	-0.740
R_C	0.211	0.639	-1.000
I_C	0.281	0.536	-1.223

*$\Delta T = 1200K$

For the geometric spot modeling and spot-temperature determination, we used our own computer programs based on Budding's (1977) equations. We applied only two-spot models with circular spots that not only fitted all light curve shapes very well but also contain a minimum of assumptions. Solutions with overlapping spots were excluded, since those falsify the spot temperature value and also conflict the circular spot assumption.

Those parameters that were kept constant for the light curve modeling are listed in Table 1. Flux ratios between the spots and the photosphere were calculated using a simple blackbody approximation with $\Delta T = T_{\rm phot} - T_{\rm spot} = 1200$ K (see Sect. 4.2) and an adopted photospheric temperature for a K0 giant of $T_{\rm phot} = 4820$ K (Bell & Gustaffson 1989). Wavelength-dependent limb-darkening coefficients were taken from the tables of Van Hamme (1993).

The spot temperature was determined using suitable subsets of data (see Sect. 4.2) and was kept constant during the final modeling process. The only free parameters in our spot modeling approach are the spot sizes in terms of their radii γ_i and the spot positions in longitude λ_i and latitude β_i ($i = 1, 2$).

Sect. 4.1 describes in detail how we determined the unspotted brightness in different wavelengths.

3.2. Phase-series light curve modeling

For most of our data we formed individual light curves phased with Eq.1. Budding's (1977) equations were used to model the light variability and a grid-search method (GSM) was applied to fit the observations. We adopted a pre-determined global unspotted magnitude throughout the modeling (see Sect. 4.1). Additionally, in order to compare the results with previous studies, the entire analysis was also carried out using the local brightness maximum as the unspotted light level for each individual light curve (see Sect. 5.2).

3.3. Time-series light curve modeling

Many of the data sets show strong cycle-to-cycle variations. To analyse these short-term variations, a new computer code was developed by one of us (Bartus 1996) for time-series spot modeling (see also paper I). Such an approach allows us to follow the changes of the spot parameters on timescales close to or even shorter than the rotational period. This approach uses the same fixed set of parameters of Table 1. Four of the data sets were solely analysed with this method because the very strong variability of the light curve shape since in those cases it is difficult to phase the data together.

Our new computer program fits Budding's (1977) equations with the help of the Levenberg-Marquardt method (LMM) (see, e.g., in Bevington 1969). We obtain the spot parameters as well as their estimated errors and linear correlation coefficients. The latter show a strong correlation among the spot parameters even in the case of our simplifying two-spot assumption (for details see Bartus 1996). The program works along the time domain in the following way: reads a pre-set time span of data points, models them as a phase curve and then steps forward in time with a stepwidth given in phase units. Because of the strong correlation among the spot parameters, it is inadvisable to introduce additional free parameters. Therefore, we did not include any parametric function to describe the migration of the spots, e.g., due to differential rotation. This implicitly assumes that the spot parameters do not change during the time span actually modeled: a constraint that can be balanced by choosing a close to 1.0-phase span (a single stellar rotation) but a small stepwidth.

3.4. Reliability of the results

No notable differences in the resulting parameters were found in spite of the entirely different approaches (phase-series and time-series modeling) and minimization techniques (GSM and LMM).

We performed a statistical test on the reliability of the modeling results by simulating the observational scatter. Fifty test light curves were generated with photometric noise between 0.0–3.0% for each 0.1% step (altogether 1500 artificial light curves) and then recovered with the approach described in Sect. 3.2. As the initial spot configuration, we used the average spot parameters for HK Lac from Table 3 and the other fixed parameters from Table 1. For the details of this test method see Kővári (1995) and Kővári & Bartus (1997). The results are displayed in Fig. 1. From this figure it seems clear that, for scatter above 0.5% in intensity ($\approx \pm 0\overset{\mathrm{m}}{.}005$), the longitude of the northern spot becomes unstable ($\sigma_{\lambda_1} > 8°$) because of its high latitude. The latitude, and even more the size of the southern spot cannot be determined with good accuracy ($\sigma_{\gamma_2} > 5°$) since usually most of that spot is not seen at all. Using the time-series spot model program this effect is well seen by the increased error bars of the results (see Fig. 10). Fortunately, most of our data have a scatter close to $\pm 0\overset{\mathrm{m}}{.}005$ or less, especially since the APT is continuously watched in its performance (Henry 1995b).

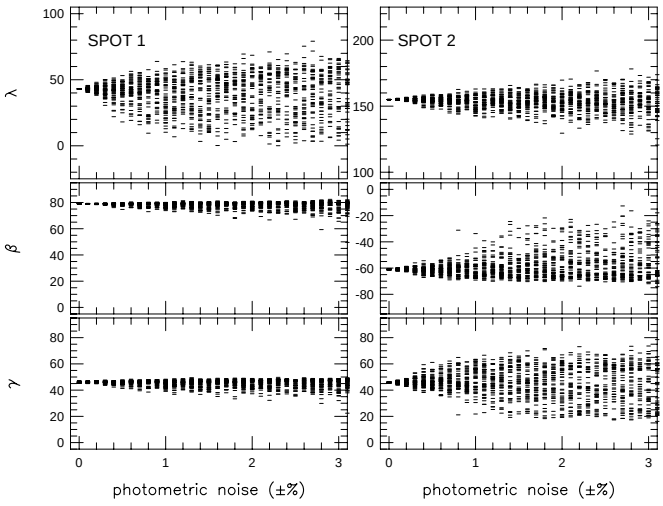

Fig. 1. Testing the reliability of the resulting spot parameters. (λ is the longitude, β the latitude, and γ the spot radius). See explanation in the text

4. Determination of the unspotted brightness and the spot temperature

4.1. Unspotted brightness

The determination of the unspotted brightness is of crucial importance in spot modeling. Its values in different colours have direct influence on the derived spot sizes and, therefore, on the calculated total spottedness of the star. The resulting spot latitudes also depend on the unspotted brightness. Information on spot latitudes is important from a theoretical point of view, although they are less well determined observationally.

However, in spite of having a long series of photometry, finding the unspotted magnitude is still problematic. Usually, either the highest brightness ever observed (e.g. Strassmeier & Oláh 1992) or the local maximum of a given light curve is used (e.g. Oláh et al. 1991). In this paper we establish the unspotted light level of HK Lac in $BV(RI)_C$ by using all existing photometry and adding our previous experience on the chromospheric activity of this particular star (Oláh et al. 1992).

Fig. 2 shows a general trend between the light curve amplitude and the brightness of the star in the sense that the larger the light curve amplitude the fainter the star at minimum light. When the unspotted level is reached, then the light amplitude is obviously zero and the star is brightest. However, the light amplitude can also be small (or zero) when the star is faint. When the light curve *minimum* is shallow (i.e. the star is bright), it suggests a lower level of spottedness. That is not true for the light curve *maximum*, since big spots can still rotate completely (or nearly completely) out of view, still showing a bright maximum while the star is heavily spotted.

By comparison, Henry et al. (1995) analysed four active stars (λ And, σ Gem, II Peg, V711 Tau) on a long term base. Looking at their Figs. 27–30, which show the stars' amplitudes vs. minimum, maximum, and mean light, one can see that in all four cases the minimum light vs. amplitude diagram shows a trend of

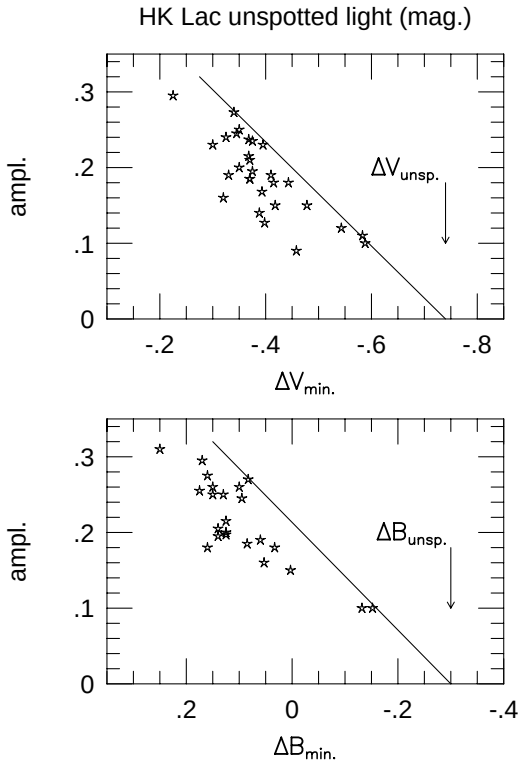

Fig. 2. The determination of the unspotted brightness of HK Lacertae. The intersection of the upper boundary line with the x-axis gives an estimation of the unspotted magnitude

Table 2. Unspotted colour indices

Color	observed	dereddened	synthetic
$B-V$	1.032	0.936	0.950
$V-R_C$	0.592	0.524	0.527
$V-I_C$	1.137	1.006	0.980

lower amplitudes with higher stellar brightness. In the cases of maximum and mean light, respectively divergent behaviour of the four stars is observed. Performing simulations, using several thousands of artifical light curves, we found a nearly linear relation between the amplitude and the minimum light as long as the photometric amplitude remains small. The unspotted values in Table 1 are from the intersection of the extrapolated (hand-drawn) upper boundary of the minimum amplitudes in Fig. 2. We found the unspotted ΔV magnitude to be $-0\overset{\mathrm{m}}{.}74$.

A similar correlation between the Mg II h&k line fluxes (a chromospheric activity indicator) and the V magnitudes was observed on HK Lac: higher Mg II flux corresponded to lower stellar brightness (Oláh et al. 1992). We suspected that when there is no Mg II line emission, no chromospheric activity is present. The unspotted ΔV magnitude obtained in this way was $-0\overset{\mathrm{m}}{.}86$.

The results purely from photometry and purely from spectroscopy differ by $0\overset{\mathrm{m}}{.}12$ from each other. The uncertainty of the unspotted brightness deduced from the Mg II line fluxes, however, is much higher (see Fig. 8 in Oláh et al. 1992). Our new unspotted brightness estimated from photometry does not necessarily contradict the result given there, because the slope of the fit can easily change due to the scatter of the Mg II fluxes fitted. On the other hand, our new value based on photometry should be considered as a minimum value for the unspotted brightness because an upper boundary was extrapolated (Fig. 2).

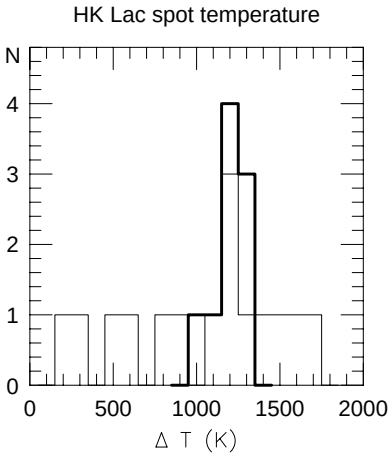

Fig. 3. Distribution of calculated spot temperatures. Thin line: two-spot results; thick line: one-spot results. N is the number of solutions obtained corresponding to a given temperature value

We have performed an independent test for the accuracy of our deduced unspotted brightness of HK Lac: with the calibrations of Bessell (1979) we calculated synthetic colour indices for HK Lac using its spectral type of K0III and compared them with our calculated unspotted values. Color indices for the comparison star (HD 210731) of $B-V$ = 0.592, $V-R_C$ = 0.332 and $V-I_C$ = 0.654 were taken from Eaton (1985). The results are given in Table 2. The synthetic colour indices are found to be systematically bluer by a similar amount. Adopting a reddening of $A_V = 0\overset{\mathrm{m}}{.}35$ in the direction of HK Lac, in agreement with the strong interstellar absorption at Mg II h&k (Oláh et al. 1992), we reproduce the synthetic colour indices within a few hundredths of a magnitude (deviations are less than $0\overset{\mathrm{m}}{.}03$).

4.2. Spot temperatures

We run solutions for $V-I_C$ and $B-V$ colour indices, separately for the colours, using ΔT values between 100–2000 K with 100 K steps. The two sets of resulting spot parameters were then averaged and the corresponding colour index curves again fitted but using the average parameters and the goodness of fit (χ^2) was calculated for each trial temperature. For the method see Strassmeier & Oláh (1992).

We found that, when the light curves were asymmetric or even double humped, the resulting temperatures exhibited large scatter, ranging between 200–1600 K. On the other hand, we had seven B and V light curves of symmetric shape (two of them were also observed in I_C), which could be fitted with one spot only. The one-spot solution has advantages. The most

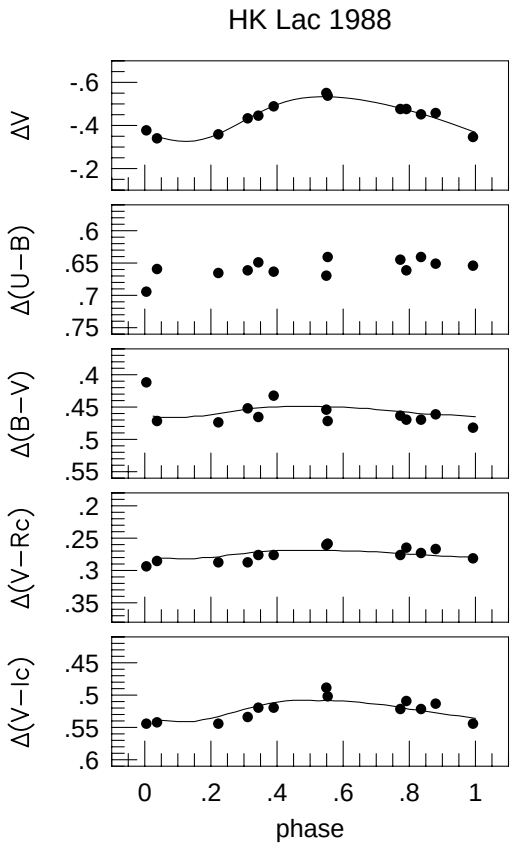

Fig. 4. Light and colour-index curves of HK Lac from 1988 and the respective fits using ΔT = 1200 K

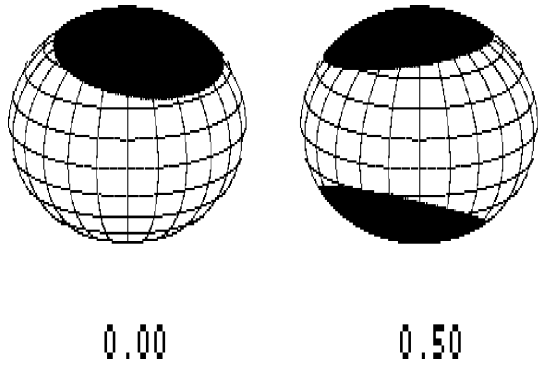

Fig. 5. Our bipolar-cap model of HK Lac at two phases (0.00 and 0.50). The average spot parameters were taken from Table 3

important is that the number of free parameters is reduced to three. Finally, these light and color curves were used for the temperature calculations. Spot temperatures for one-spot and two-spot solutions are displayed in the histogram in Fig. 3 and show a strong peak around ΔT = 1200 $\pm$ 100 K. The 1988 light curve is displayed in Fig. 4 as an example.

Previous spot temperature determination of HK Lac by Vogt (1981) resulted in ΔT = 950 $\pm$ 200 K using V and R light curves and the Barnes-Evans surface brightness relation. This

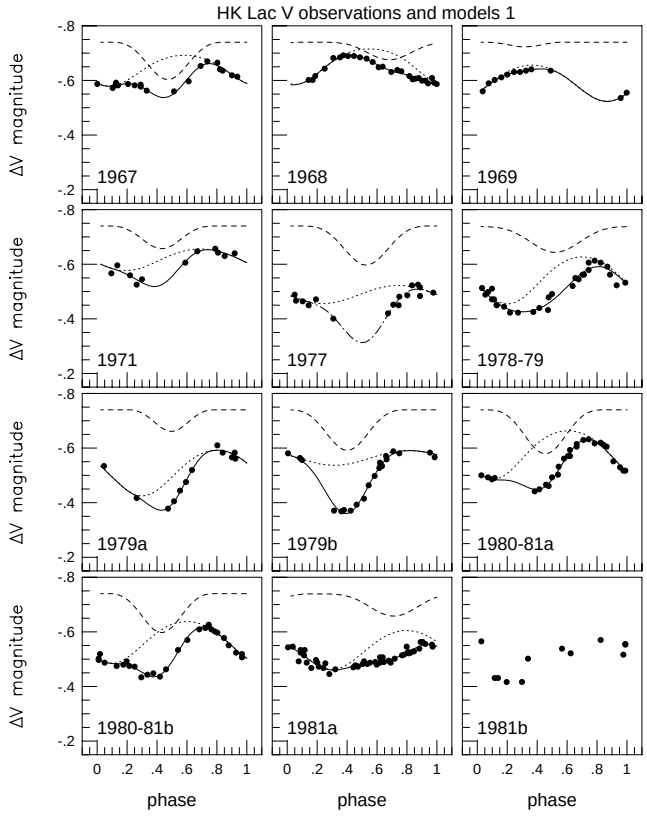

Fig. 6. Phase-series of V light curves of HK Lac (dots) and the respective two-spot fits with the model shown in Fig. 5. Light loss caused by the northern and southern spots are displayed by dotted and dashed lines, respectively. The fits to the data are drawn as continuous lines and, in the case of insufficient data coverage, by a dash-dotted line

value was considered a lower limit, since it refered to a least spotted hemisphere rather than to an immaculate one. Later, Poe & Eaton (1985) calculated ΔT = 1200 K from $V - I_C$ observations with a method similar to that of Vogt (1981).

5. Light curve modeling

5.1. Resulting spot parameters

All fits to the V light curves are displayed in Fig. 6. With the derived unspotted brightness our modeling code could only satisfactorily fit the complete data set when two polar spots, located near the north *and* the south rotation poles, are used. As noted in Sect. 4.1, the derived unspotted brightness should be considered as minimum value. The polar spot solution breaks when the unspotted brightness is lower by a few hundredths of magnitude than given in Table 1. Pre-defined non-polar spot configurations were tested and found to yield unsatisfactory fits to all the data. The magnitude range to be fitted is very large because of the large amplitude variations at low stellar brightness (e.g. a $0\overset{\mathrm{m}}{.}25$ amplitude at a light curve maximum $0\overset{\mathrm{m}}{.}25$ below the unspotted brightness). In Fig. 5 we show the average spot configuration on HK Lac from 30 years of data (as given in Table 3).

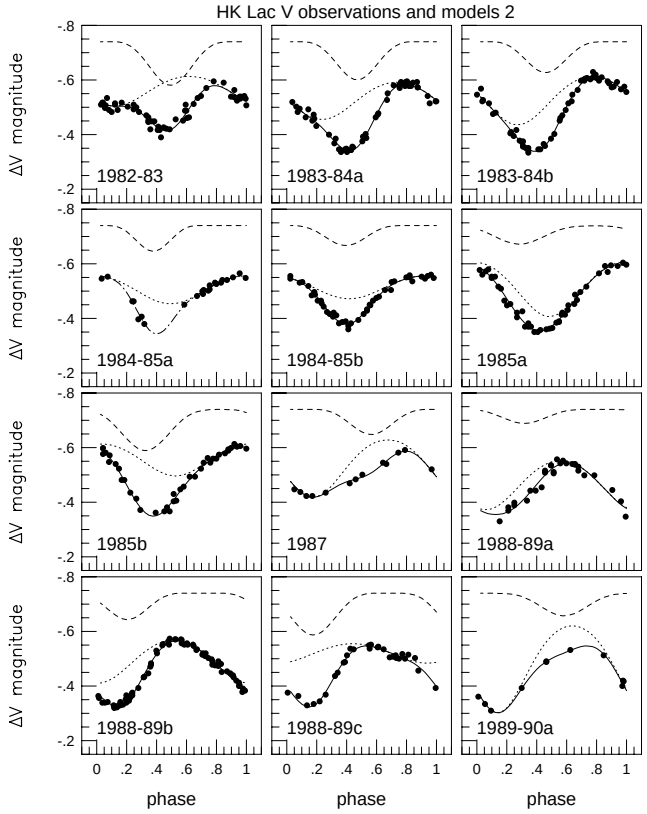

Fig. 6. (continued)

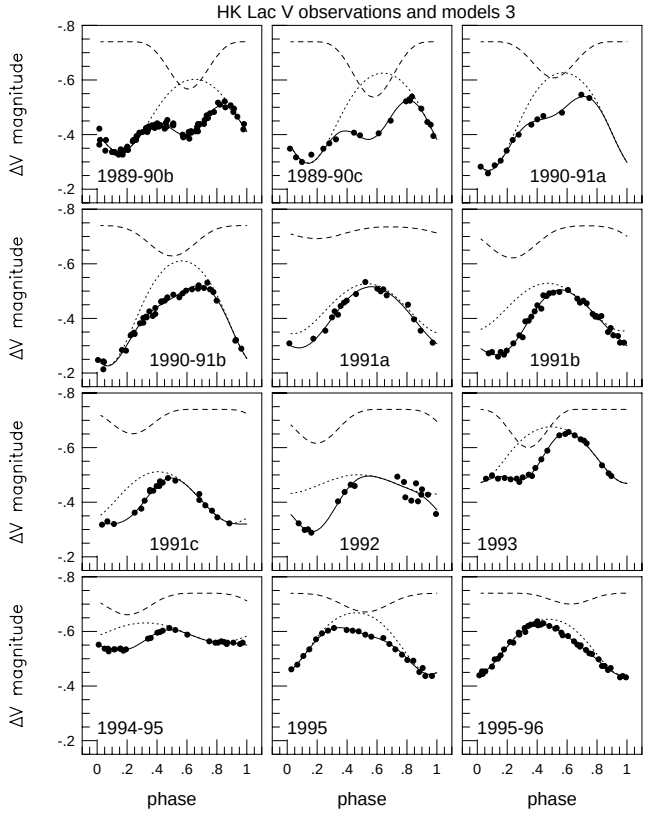

Fig. 6. (continued)

Table 3 gives the spot solutions for the 34 phased light curves fitted with two polar spots. The first column gives the mean J.D. of the observations, the next six columns contain the spot longitudes expressed in orbital phases and the spot latitudes and radii for the two spots, respectively. Finally, in the last column, the spot coverage of the total stellar surface is given in percents. The last two rows in Table 3 are the average spot parameter values and their respective standard deviations.

Fig. 7 summarizes our results on the long-term spot variability of HK Lac. The upper three panels combine all observational data in V, $B-V$, and $U-B$, respectively. One year after the discovery of the light variability in 1967, the star was at its highest brightness ever observed: $\Delta V_{\rm max} = -0\overset{\rm m}{.}69$ (Blanco & Catalano 1970). We have no data between 1971–1977 but the average brightness of the star seemed to have decreased considerably. Between 1977–1988 the mean brightness was nearly constant at about $\Delta V_{\rm mean} = -0\overset{\rm m}{.}49$. A sudden decrease of the mean light level began in 1989, and by 1991 HK Lac was at its faintest stage ever observed ($\Delta V_{\rm min} = -0\overset{\rm m}{.}24$). This was followed by a much faster brightening which lasted only for about a year. From 1993 until 1994 its mean light level has remained high ($\Delta V_{\rm mean} = -0\overset{\rm m}{.}56$), though not as high as between 1967–1971, and in 1995 decreased again to $\Delta V_{\rm mean} = -0\overset{\rm m}{.}54$.

The spot coverage of HK Lac, displayed in the fourth panel of Fig. 7, naturally follows the brightness changes in the top panel. In this panel we have plotted the results obtained from the phased light curves (Table 3, last column) as dots, and from the time-series modeling as small open squares. The latter serve also as a hint of the general accuracy of average spot coverage determinations. Deviations up to 5–10% from the mean value are partly due to the internal scatter of the data ($\approx \pm 2\%$) but also reflect short-term changes of the spottedness. The spot phases, drawn in the bottom panel of Fig. 7, show systematic behaviour as well, discussed in detail in the following subsection.

5.2. Longitudinal migration of spots

As mentioned in Sect. 3, we also ran solutions using the local light maxima for each light curve as the unspotted magnitudes. In this way we can compare our results, using an absolute unspotted V magnitude, with the previous results by Oláh et al. (1991). The upper panel of Fig. 8 shows the extended version of Fig. 1 from Oláh et al. (1991). Since in this earlier analysis local maxima were used as the unspotted brightness, the overall spottedness of the star was neglected and the light variations were described by two low-latitude spots which sometimes disappeared and new ones emerged. The lines connect phase positions of a given spot during its suggested lifetime. Positions marked with C, D, and E, represent phase discontinuities interpreted to be places of newly emerged spots (Oláh et al. 1991).

In our new approach, spotted areas account also for the variations in overall spottedness. However, sudden changes in the light curves still can be due to the emergence of new spots, but

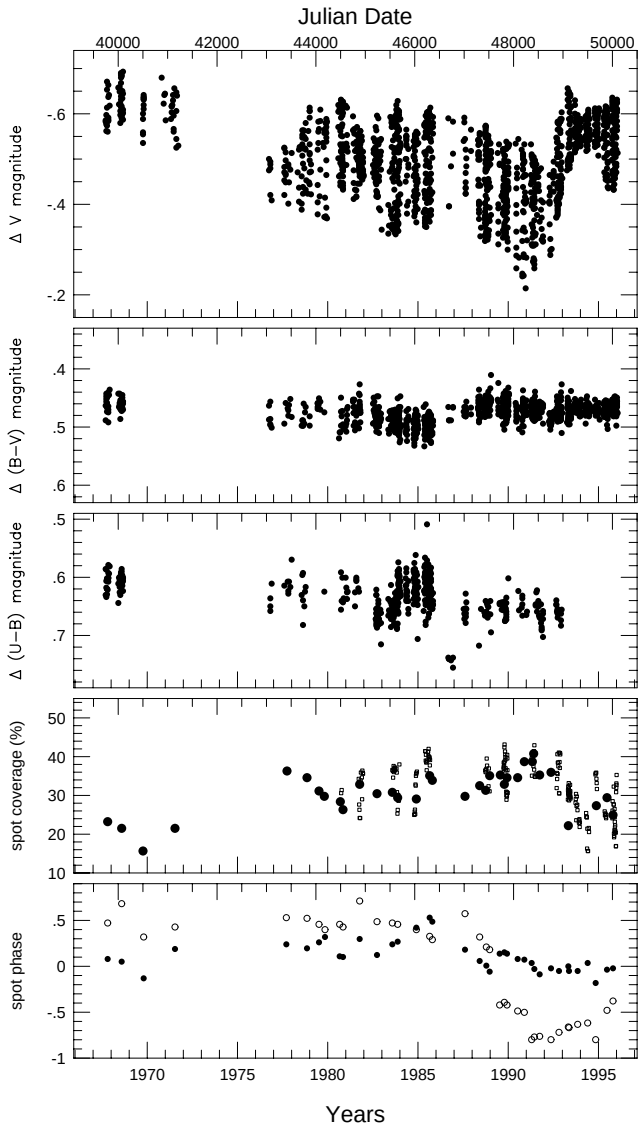

Fig. 7. Long-term observed variability of HK Lac between 1967–1996. The upper three panels display all photometric observations in V (the top border of the box corresponds to the unspotted brightness), $B-V$, and $U-B$. The fourth panel gives the spot coverage in percents (dots: phase-series results; open squares: time-series results) and the bottom panel shows the phases of the active-region centers (dots: northern; circles: southern polar region

within an already active region, thereby shifting its centre, which appears as a phase discontinuity in the phase-time diagram. In the lower panel of Fig. 8 we give the central phases of the polar active regions. For comparison, we connect the phase positions of the polar active regions with dashed lines in the lower panel as well. Thus, one can clearly distinguish between the northern and southern active regions all the time. As expected, the longitudinal migration and phase discontinuities of the polar active regions are very similar as obtained for the low-latitude spots before.

Table 3. Resulting spot parameters

J.D.	λ_1	λ_2	β_1	β_2	γ_1	γ_2	area
average	(orbital phases)		(degrees)		(degrees)		(%)
39785	0.08	0.47	78	−54	33.5	45.3	23.1
40075	0.05	0.68	72	−68	30.1	45.1	21.4
40512	−.13	0.32	79	−59	39.8	23.7	15.8
41146	0.19	0.43	83	−56	37.1	39.2	21.4
43405	0.24	0.53	86	−59	50.5	50.4	36.3
43815	0.20	0.52	78	−71	44.9	53.3	34.7
44064	0.26	0.46	82	−58	45.8	47.3	31.2
44182	0.32	0.40	86	−55	43.5	47.2	29.8
44483	0.11	0.46	76	−53	40.8	47.5	28.4
44544	0.10	0.43	79	−49	42.9	42.3	26.4
44886	0.30	0.71	81	−70	45.9	49.8	32.9
45237	0.12	0.49	83	−54	43.7	48.2	30.6
45539	0.24	0.47	82	−54	47.0	45.5	30.9
45653	0.27	0.46	78	−56	46.5	43.4	29.3
46026	0.42	0.40	85	−61	48.3	41.3	29.2
46295	0.53	0.33	82	−64	44.0	54.7	35.1
46355	0.49	0.29	78	−72	48.0	49.2	33.9
47018	0.18	0.57	77	−61	46.2	44.6	29.8
47313	0.06	0.32	81	−69	52.1	42.8	32.6
47444	0.01	0.21	81	−58	50.0	43.0	31.3
47511	−.06	0.18	86	−59	47.8	51.2	35.1
47722	0.14	0.58	73	−68	50.6	48.8	35.3
47815	0.15	0.61	75	−48	50.6	45.1	33.0
47869	0.14	0.58	72	−48	50.5	47.9	34.7
48075	0.08	0.51	71	−57	51.2	47.0	34.6
48220	0.07	0.50	71	−66	53.4	51.0	38.7
48371	0.04	0.20	81	−79	54.3	49.9	38.8
48417	−.03	0.23	81	−67	53.8	53.6	40.8
48528	−.09	0.24	81	−60	55.6	43.2	35.3
48765	−.02	0.20	86	−60	52.4	48.1	36.1
49101	.00	0.34	73	−43	40.4	37.2	22.1
49664	−.18	0.20	84	−67	39.8	46.9	27.4
49896	−.04	0.52	73	−71	42.2	48.1	29.5
50013	−.02	0.62	76	−67	44.3	38.3	25.0
average	0.12	0.43	79	−61	46.1	45.9	30.9
±	0.17	0.15	5	8	5.9	5.7	5.6

From Table 3 and Figs. 5, 7, and 8 it is also seen that active-region centers tend to stay at certain active longitudes on the stellar surface, around orbital phases of 0.12 (43°) and 0.43 (155°), respectively. Fig. 9 displays the longitude distributions of the polar caps. The separation between the two active longitudes is 112°±40° within the 30 years of observations. The same value was found well within 1σ (102°±25°) from the first 17 years of observations (see Oláh et al. 1986).

5.3. Time-series results

Altogether, 17 data segments were suitable for time-series spot modeling, having adequate coverage of data points for more than three consecutive cycles. In Fig. 10 six data sets are displayed. Note that the errorbars for the resulting parameters are the highest where the phase coverage is poorest.

The first data set from 1981 was observed shortly after strong phase discontinuities of both polar caps appeared in

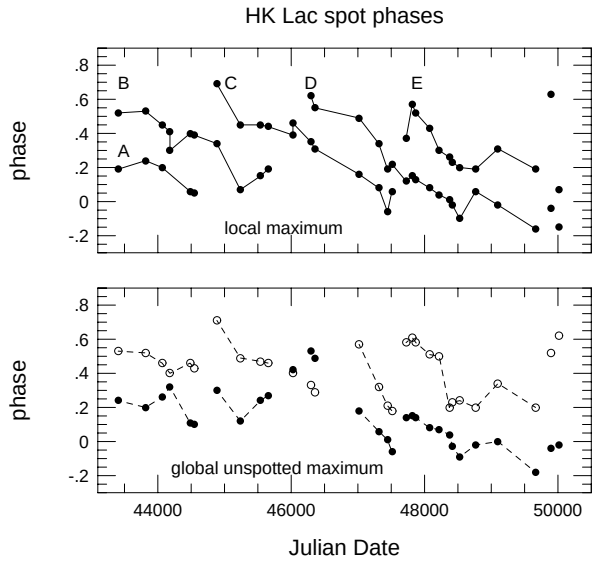

Fig. 8. Phases of the centers of active regions on HK Lac. Upper panel: if local maxima are used as the unspotted brightness (as in Oláh et al. 1991); lower panel: present results (dots mark the northern, circles the southern polar active region). Further descriptions are given in the text

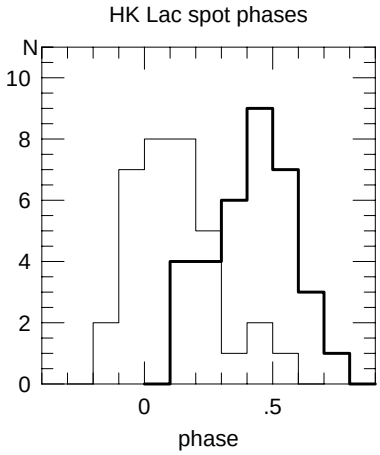

Fig. 9. Histogram of the spot longitudes. Thin line: northern active region; thick line: southern active region. N is the number of phase values at a given phase range

1980 (see Fig. 8), probably indicating the appearence of new spots in those regions. The light curves observed in 1985, also plotted in Fig. 10, show a more smooth variation with little changes. Shortly after 1985, a continuous brightness decrease set in and, in 1989, strong variability was observed again at low system brightness. Fig. 10 also shows a continuous series of modeled light curves from 1992 through 1994. These observations demonstrate how fast, i.e. within one year, HK Lac came out from the big light depression, then reached nearly the highest brightness ever observed. In 1992 the mean light was continuously brightening, but the amplitude remained constant. From 1993 to 1994 all observed consecutive light curves show strong cycle-to-cycle variability at very high system brightness.

Table 4. Events in HK Lac between 1967–1996

Year	spottedness	mean light	remarks
1968	lowest ever	max.	close to unspotted
1971–77	increases from 20% to 36%	decr.	no observations within this time interval
1977–80	decreases from 36% to 26%	incr.	spot dissolving
1981	jumped to 33%	decr.	new spots near both poles, phase jumps
1981–84	decreases	stays	spot dissolving slow and restructuring
1984–89	jumped to 35% later increases	decr.	new spot in the north later in the south phase discontinuities
1989	increases	decr.	new spots near both poles, phase jumps transient events
1989–91	increases up to 40%	decr. fast	more spots appear
1991–92	decreases down to 20%	incr. fast	spots dissolving fast
1993–	increases	decr.	probably new spots

All the variability could easily be described by small motions and/or changes of the spotted areas, as seen in the lower panels throughout Fig. 10.

6. Discussion

In the past years spot modeling via Doppler imaging reproduced high latitude spots covering the stellar rotational pole(s), see e.g. Vogt & Hatzes (1996). Recent models on the dynamics of magnetic flux tubes clearly show that at high rotation rates and/or in case of deep convective zones, spots appear at high stellar latitudes close to the poles. For an overview of this subject see the recent review by Schüssler (1996).

Due to the strong instability of spot latitudes in photometric modeling (Kővári 1995, Kővári & Bartus 1997), one easily can find good fits to the photometric data with spots on or near the stellar poles as well. Modeling the light variability of the short-period binary ER Vul, which is composed of two solar-type stars, Oláh et al. (1994) have already raised the possibility of the polar spot scenario based on the theoretical background of Schüssler & Solanki's (1992) work on rapidly rotating dwarf stars. Although at present detailed calculations of polar spot emergence on giant stars is still underway, preliminary results show that, having deep convective zones, giant stars have the

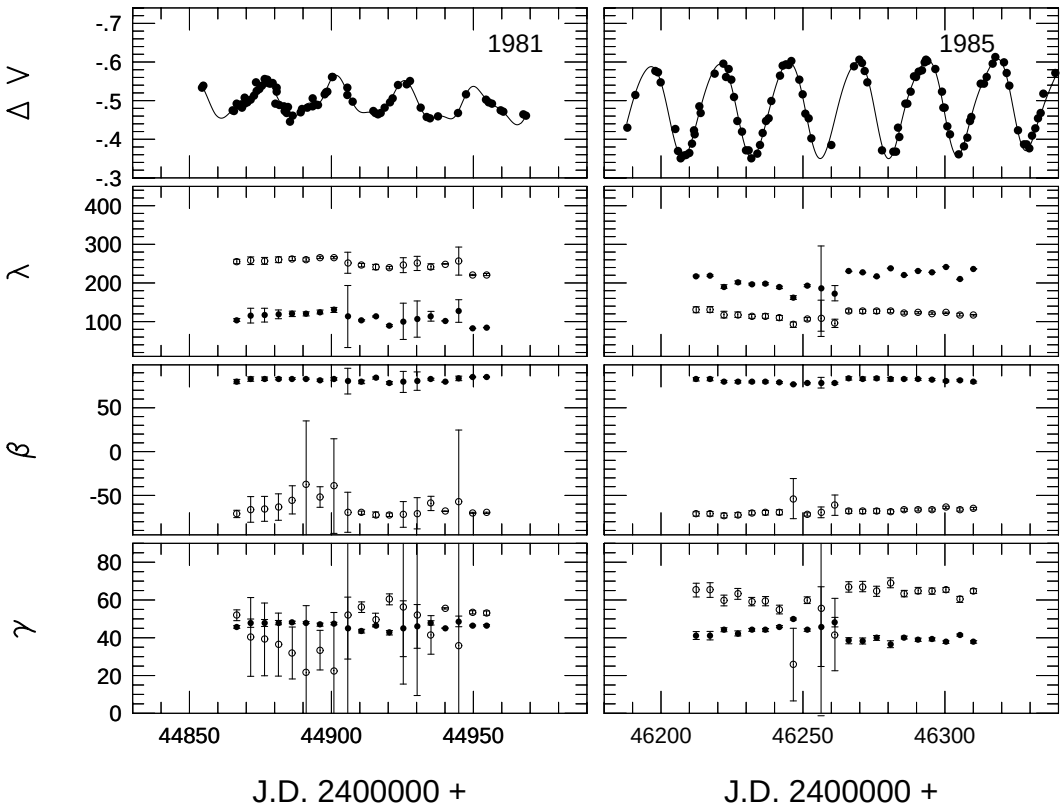

Fig. 10. Modeled light curves from two different seasons and the results from time-series spot modeling. Each diagram block consists of four panels: the upper panel shows the observations and the fit, the lower three panels give the recovered changes of the longitude, latitude and radius vs. time, respectively. Again, dots represent the northern, open circles the southern active region

necessary conditions for having very high latitude (truly polar) spots (Schüssler 1996).

Considering the following observational evidences – that *a)* HK Lac had very high amplitude variability at low system brightness and *b)* the spot temperature cannot be much lower than our suggested value – we conclude that using polar spots is the only way for a satisfactory fit of the light curve shape together with the overall light variability.

Mathematically, of course, it is possible to find an infinite number of solutions with many little spots scattered arbitrarily over the stellar surface. Using appropriate differential rotation, light curve and long term changes could also be followed satisfactorily with many random spots (Eaton et al. 1996). Nevertheless, we rejected these solutions because of the strong theoretical and observational support from Doppler imaging techniques of spotted polar regions as outlined above.

The modeling of the rise of flux tubes that leads to polar spots describes bipolar spot emergence (Schüssler 1996). Adopting this scenario, active regions on stars like HK Lac probably consist of a number of such pairs. If we relate the time when new spots appear with the positions of phase jumps (see Fig. 8 and Table 3), we might suggest that spot emergence tends to prefer phases around 0.2 and 0.7, at half stellar circumference from each other. When a new spot appears, a restructuring of the spots within an active region is observed with corresponding light curve changes. Moreover, interactions between the newly emerged spots and the old ones could be the reason for rapid changes in the observed light curves (see also Oláh et al. 1988).

7. Conclusions

1. Combining the photometric data of HK Lac from 1967 to 1996, we found substantial changes in the mean brightness as well as in the light amplitude. However, we did not detect a well-determined long-term periodic light variability according to the solar paradigm.
2. We model all photometric observations from the past 30 years with a bipolar-cap scenario consisting of two asymmetric spots near the north pole and the south pole. The two polar caps seemed to exist throughout the entire 30 years, though continuous changes in the positions and sizes of both polar caps were found.
3. On the basis of BVI_C data, we determined an average spot temperature difference of 1200 ± 100 K cooler than the photosphere, in good agreement with previous temperature determinations.
4. A new method was described that allows to establish the minimum value of the unspotted brightness level for HK Lac. Synthetic color indices also agree with those calculated with our new unspotted magnitudes.

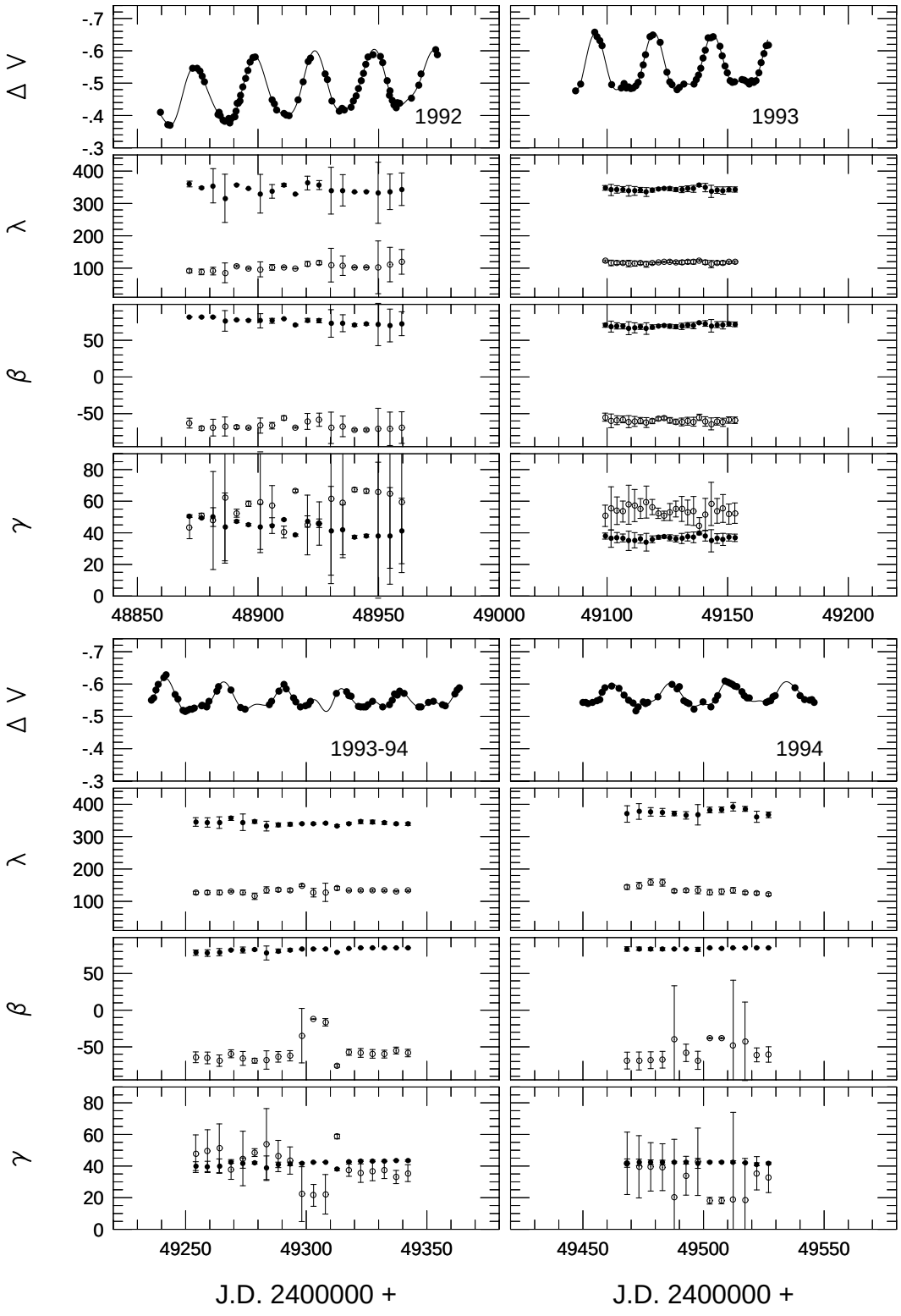

Fig. 10. (continued)

5. We apply a new time-dependent spot modeling computer code that takes into account cycle-to-cycle light curve changes of HK Lac. From this we recorded the same polar-cap scenario as from our phase-dependent spot modeling approach.
6. We tested the reliability of our results and conclude that *a)* precise photometric observations with noise level less than 0.5% are required to recover the spot parameters within $\pm 5 - 10^\circ$ in λ and $\pm 2 - 5^\circ$ in β and γ as well, and *b)* well-covered light curves are necessary for time-series modeling to avoid unreliable spot parameter changes from cycle-to-cycle.
7. The two active polar regions are separated on average by $\approx 110^\circ$ in longitude. Longitudinal positions of the polar caps calculated once with local and once with global maximum brightness agree well with each other. However, the respective latitudes do not agree. We presume that these active regions are actually places of emerging spots at times when phase discontinuities are observed.

Acknowledgements. The authors wish to thank Dr. E. F. Guinan for his helpful suggestions. Support from the Hungarian Research Grants OTKA T-015759, T-019640, F-019642 is acknowledged by KO, ZsK and JB. Research at the University of Vienna is supported by the "Austrian Fond zur Förderung der wissenschaftlichen Forschung" (FWF) through grant S7301-AST, and through grant OWP-40 from the Austrian Academy of Sciences to KGS. Automated astronomy at TSU has been supported for several years by the National Aeronautics and Space Administration and by the National Science Foundation, most recently through NASA grants NAG8-1014, NCC2-883, and NCCW-0085 and NSF grant HRD-9550561.

References

Bartus J. 1996, *Occ. Techn. Notes at Konkoly Obs. No.6*
Bell R.A., Gustaffson B. 1989, MNRAS 236, 653
Bessell M.S. 1979, PASP 91, 580
Bevington P.R. 1969, in: *Data Reduction and Error Analysis for the Physical Sciences*, McGraw-Holl Book Company
Budding E. 1977, Ap&SS 48, 207
Blanco C. Catalano S. 1970, A&A 4, 482
Catalano S., Frasca A. 1994, A&A 287, 575
Catalano S. et al. 1996, in: *Stellar Surface Structure*, IAU Symp. No. 176, eds.: K.G. Strassmeier and J.L. Linsky, Kluwer, Dordrecht, p. 403
Dempsey R.C. et al. 1993a, ApJS 86, 599
Dempsey R.C. et al. 1993b, ApJ 413, 333
Derman E., Demircan O., Kahraman G. 1990, A&AS 86, 421
Drake S.A., Simon T., Linsky J.L. 1992, ApJS 82, 311
Eaton J. A., Henry G. W., Fekel F., 1996, ApJ 462, 888
Eaton J.A. 1985, IAU Archive of unpublished data, file No. 147
Estalella R. et al. 1993, A&A 268, 178
Fernández-Figueroa M.J. et al. 1994, ApJS 90, 433
Gorza W.L., Heard J. F. 1971, Pub. DDO 3, 107
Henry G.W. 1995a, in: *Robotic Telescopes*, eds: G.W. Henry and J.A. Eaton, PASPC 79, p. 37
Henry G.W. 1995b, in: *Robotic Telescopes*, eds: G.W. Henry and J.A. Eaton, PASPC 79, p. 44
Henry G.W. et al. 1995, ApJS 97, 513
Herbst W. 1973, A&A 26, 137
Kővári Zs. 1995, in: *Stellar Surface Structure, Poster Paper Proc.*, IAU Symp. No. 176, ed.: K.G. Strassmeier, p. 21
Kővári Zs., Bartus J. 1997, A&A, accepted
Mitrou C.K. et al. 1995, A&AS 115, 61
Oláh K. et al. 1985, Ap&SS 108, 137
Oláh K. et al. 1986, Astrophys. Letters 25, 133
Oláh K., Gesztelyi L., Holl A. 1988, Proc. 10th ERAM of the IAU, ed. P. Harmanec, *Publ. Astr. Inst. Czech. Acad. Sci.* No. 70
Oláh K., Hall D.S. 1988, Comm. Konkoly Obs. No. 92
Oláh K., Hall D.S., Henry G.W. 1991, A&A 251, 531
Oláh K. et al. 1992, MNRAS 259, 302
Oláh K. et al. 1994, A&A 291, 110
Percy J. R., Welch D. L. 1982, JRAS Canada 76, 185
Poe C. H., Eaton J. A. 1985, ApJ 289, 644
Schmidt-Kaler T. 1982, in: *Landolt-Börnstein Vol. 2b*, eds. K. Schaifers and H.H. Voigt, Springer-Verlag Berlin-Heidelberg-New York, p.1
Randich S., Giampapa M.S., Pallavicini R. 1994, A&A 283, 893
Schüssler M. 1996, in: *Stellar Surface Structure*, IAU Symp. No. 176, eds.: K.G. Strassmeier and J.L. Linsky, Kluwer, Dordrecht, p. 269
Schüssler M., Solanki S.K. 1992, A&A 264, L13
Stawikowski A., Glebocki R. 1994, Acta Astr. 44, 393
Strassmeier K.G., Bopp B. W. 1992, A&A 259, 183 (paper I)
Strassmeier K. G., Hall. D. S., Henry G. W. 1994, A&A 282, 535 (paper II)
Strassmeier K.G., Oláh K. 1992, A&A 259, 595
Strassmeier K.G. et al. 1993, A&AS 100, 173
Van Hamme W. 1993, AJ 106, 2096
Vogt S.S. 1981, ApJ 250, 327
Vogt S.S., Hatzes A.P. 1996, in: *Stellar Surface Structure*, IAU Symp. No. 176, eds.: K.G. Strassmeier and J.L. Linsky, Kluwer, Dordrecht, p. 245

This article was processed by the author using Springer-Verlag LaTeX A&A style file *L-AA* version 3.